

Vibrational spectra of ferrocene, ferrocene-containing polymers and their oxidized compounds

Markus Appel^{1,2}, Bernhard Frick¹, Alexandre Ivanov¹,
Johannes Elbert³, Matthias Rehahn³, Markus Gallei³,
Tinka Luise Spehr² and Bernd Stühn²

¹ Institut Laue-Langevin, 71 avenue des Martyrs, 38000 Grenoble, France

² Institute of Condensed Matter Physics, Technische Universität Darmstadt,
Hochschulstraße 8, 64289 Darmstadt, Germany

³ Ernst-Berl Institute for Chemical Engineering and Macromolecular Science, Technische
Universität Darmstadt, Alarich-Weiss Straße 4, 64287 Darmstadt, Germany

E-mail: appel@ill.eu

Abstract. Ferrocene-containing polymers are an important member in the class of redox-responsive polymers, changing e.g. their solubility or conformation upon external stimuli. We present a study of their vibrational spectra using inelastic neutron scattering, focusing on the central building block of these polymers, the organometallic ferrocene complex. The vibrational modes of a bulk ferrocene sample are compared to those of poly(vinylferrocene), poly(ferrocenyldimethylsilane) and poly(ferrocenylmethylsilane). In the former polymer, the ferrocene complex is laterally attached to the polymer chain and the vibrational spectrum shows a slight shift and broadening of the fingerprint modes in the range of 100–800 cm⁻¹, except for the ring-metal-ring stretching mode which was not detectable anymore. The latter two polymers, where the ferrocene complex is part of the polymer backbone, exhibit larger differences to the vibrational spectrum of bulk ferrocene. Moreover, several contributions to the spectra caused by methyl groups in these polymers could be identified. In order to study the influence of oxidation on ferrocene and redox-responsive polymers, we investigated the ionic compound ferrocenium triiodide and oxidized poly(vinylferrocene). It is observed that the weakening of the η^5 -complex bond by a missing electron leads to a significant shift of the fingerprint modes to lower frequencies.

1. Introduction

In the last decade stimuli-responsive polymers, which are able to alter their solubility, conformation or form/break covalent bonds upon an external trigger have attracted enormous attention [1–4]. Beside the vast majority of reports on temperature, light or pH responsive materials, other external triggers are also of growing interest [2, 5]. One of these less studied triggers is the redox-stimulus [6, 7]. Redox-responsive polymers can be produced, for example, by incorporating redox active organometallic sandwich complexes in the polymer [8, 9]. The most widely used organometallic building block is ferrocene, due to the excellent combination of redox, mechanical, semi-conductive, photo-physical and opto-electronic properties in the polymers formed [10–12]. For example, these polymers have been used in composite colloidal crystal films [13], self-healing materials [14] for redox-responsive release from nanocapsules [15], for switching surface wettability [16], for modulating the activity of catalysts [17] or for



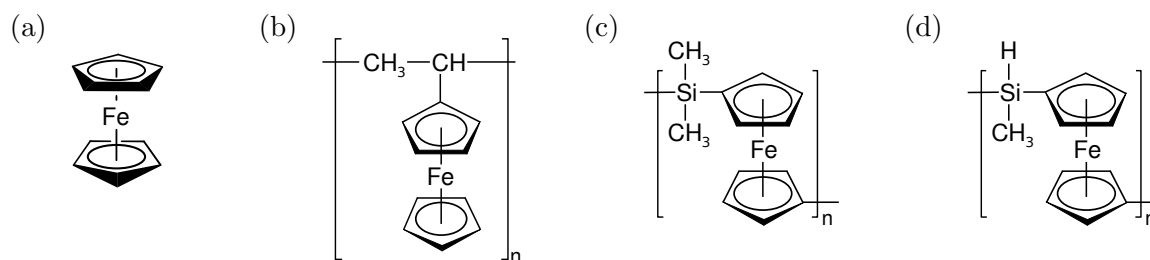


Figure 1. Chemical structure of (a): the ferrocene (Fc) molecule, and the ferrocene-containing polymers (b): poly(vinylferrocene) (PVFc), (c): poly(ferrocenyldimethylsilane) (PFDMS), and (d): poly(ferrocenylmethylsilane) (PFMS).

ion-selective membrane-gating [18]. In addition a vast amount of block copolymers with the ferrocene in the main chain, e.g., poly(ferrocenyldimethylsilanes), or with laterally bound ferrocene, e.g., poly(vinylferrocene), have been synthesized and their self-assembly in bulk and solution has been studied [10, 19–28].

Although many applications of these polymers have been explored, fundamental understanding of the local dynamics of ferrocene in these polymers and how it is influenced by oxidation is rather limited. With our experiments presented here, we aim to investigate the vibrational properties of the ferrocene moieties when incorporated in the macromolecular structure of polymers and/or being subject to oxidation. Vibrational spectroscopy using inelastic neutron scattering (INS) on ferrocene has been proven useful in previous studies of the interactions of isolated ferrocene molecules in supercages of zeolite [29, 30]. We now apply INS to compare the vibrational modes in bulk ferrocene, shown in figure 1(a), to different ferrocene-containing polymers. In poly(vinylferrocene) (PVFc), shown in figure 1(b), the ferrocene moiety is laterally attached to the polymer chain as side group, where poly(ferrocenyldimethylsilane) (PFDMS), shown in figure 1(c), contains ferrocene as part of the polymer backbone. In order to separate the influence of the methyl groups in PFDMS, we additionally include poly(ferrocenylmethylsilane) (PFMS) shown in figure 1(d) in our study. Here, one out of the two methyl groups per monomer moiety is substituted by a hydrogen.

For better understanding of the redox-responsiveness of these polymers, we investigated the effect of oxidation on the vibrational properties of ferrocene and ferrocene-containing polymers. We first compare bulk ferrocene to ferrocenium triiodide salt and subsequently study PVFc after oxidation with iodine.

2. Experimental

Ferrocene was purchased from Alfa Aesar (purity 99%) and used without further purification. Ferrocenium triiodide (FcI_3) was obtained by stoichiometric mixing of ferrocene and iodine in dichloromethane and subsequent evaporation of the solvent yielding a black powder.

PVFc (20 kg mol^{-1}) [31], PFDMS (16 kg mol^{-1} and 88 kg mol^{-1}) [32] and PFMS (28 kg mol^{-1}) [33] were synthesized by anionic polymerization according to procedures described in literature. The molecular weights of the obtained polymers were determined by gel permeation chromatography (GPC). In order to obtain oxidized PVFc, 213 mg (0.84 mmol) iodine were added to a solution of 177 mg PVFc (0.84 mmol corresponding to ferrocene units) in 10 ml THF. After 1 h, 80 ml diethyl ether were added to precipitate the oxidized polymer. 250 mg oxidized PVFc is obtained after washing with diethyl ether and drying in vacuo. As the distribution and character of the iodine counterions (e.g., I^- or I_3^-) was not investigated further, we refer to the oxidized compound as PVFcI_x .

Vibrational spectra were recorded on the hot neutron spectrometer IN1-Lagrange at the

Institut Laue-Langevin, Grenoble (France). For the neutron scattering experiments the powder samples of FcI_3 and PVFcI_x were packed in aluminum foil and rolled into a hollow cylinder of ≈ 15 mm diameter. The remaining samples (Fc, PVFc, PFDMS16, PFDMS88, PFMS) were loaded in 3×4 cm flat aluminum containers of 0.3–0.5 mm thickness. All experiments were performed at a sample temperature of $T = 10$ K controlled by a standard closed-cycle He cryostat. The incident neutron energy E_i was varied by scanning the Bragg angle of different monochromator reflections: Si(111) (5–22 meV), Si(311) (17–70 meV) and Cu(220) (40–500 meV). The downward scattered neutrons from the sample are selected at fixed $E_f = 4.5$ meV and focused on a single detector by a large area PG(002) analyzer covering scattering angles 2θ in the range ≈ 21 – 159° . A typical energy resolution was ≈ 2 – 4% in energy transfer $\hbar\omega = E_i - E_f$ depending on the selected monochromator reflection and E_i . Scattering from the empty cell was subtracted, and the recorded intensity was normalized and corrected for energy dependent monitor efficiency. Subsequently, correction factors from a water sample measurement were applied to compensate for a minor dependency of the monitor flux on the monochromator take-off angle. The resulting intensity is proportional to the dynamic structure factor $S(Q, \omega)$ of the sample, where the magnitude of the scattering vector Q depends on ω and the scattering angle 2θ which is sampled over the whole 2θ -range covered by the analyzer. Finally, from the relationship [34]

$$G(\omega) \propto \frac{\omega}{Q^2} S(Q, \omega) \left(1 - e^{-\hbar\omega/k_B T}\right) \quad (1)$$

the generalized density of states $G(\omega)$ is calculated and will be discussed further in this paper.

3. Results & Discussion

In the following, we will present the vibrational spectra collected in this study. We start with a comparison of bulk Fc in its triclinic crystalline phase and various ferrocene-containing polymers. Subsequently, we turn to the effect of oxidation and discuss the oxidized compounds FcI_3 and PVFcI_x .

3.1. Ferrocene and Ferrocene-containing polymers

The vibrational spectra of triclinic Fc and different ferrocene-containing polymers is shown in figure 2. Vertical lines correspond to maxima in the Fc spectrum for easier comparison. The spectrum for Fc (shown in the bottom part of figure 2) exhibits collective lattice modes in the low energy range up to 100 cm^{-1} as well as local molecular excitations at higher frequencies. It compares well to previous INS measurements published by Kemner *et al.*, where a detailed discussion, assignment and visualization of the individual modes is given [29]. The sketch below the graph in figure 2 indicates the displacements associated with the modes between 180 cm^{-1} and 595 cm^{-1} . The broadened, intense peak structure at higher frequencies between 800 and 1100 cm^{-1} is caused by several modes involving internal distortions of the cyclopentadienyl (Cp) rings and has been analyzed in more detail by Kemner *et al.* [29].

Compared to crystalline ferrocene, the spectrum of amorphous PVFc in the middle part of figure 2 shows less detail as expected. However, for this polymer, we expect the vibrational spectrum to bear the most resemblance to bulk Fc as the ferrocene moieties are attached laterally as side chain by a single C—C bond. Indeed the modes at 390 , 484 , 500 and 595 cm^{-1} are clearly distinguishable in the spectrum of PVFc, and only the mode at 500 cm^{-1} shows a slight shift to higher frequencies and the mode 595 cm^{-1} a slight shift to lower frequencies with respect to bulk Fc. The mode at 180 cm^{-1} corresponding to ring-metal-ring bending with antisymmetric ring tilt is also slightly shifted to lower frequencies and broadened in PVFc. The superposition of multiple modes mostly involving ring distortion and C—H bending leading to the 4 broad peaks between 800 and 1100 cm^{-1} appear even more smeared in PVFc, but not shifted.

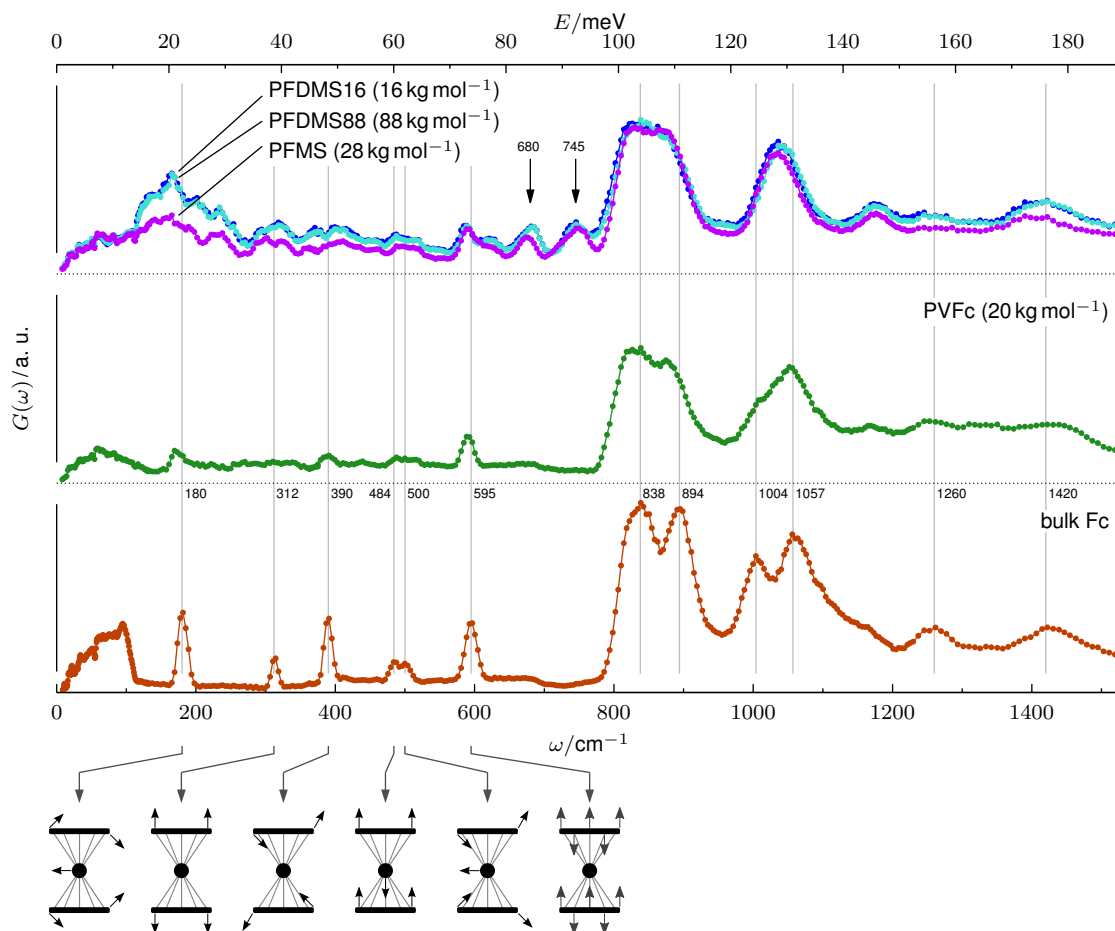


Figure 2. Experimental generalized density of states $G(\omega)$ for triclinic ferrocene (Fc), poly(vinylferrocene) (PVFc), poly(ferrocenyldimethylsilane) (PFDMS) with two molecular weights, and poly(ferrocenylmethylsilane) (PFMS). All spectra were recorded at $T = 10$ K. Vertical lines show characteristic maxima of the Fc spectrum for easier comparison (ω given in cm^{-1}). The sketch below the graph indicates the type of distortion associated with some fingerprint modes of the ferrocene molecule.

Interestingly, the mode at 312 cm^{-1} is not easily visible in the spectrum of PVFc. This mode corresponds to ring-metal-ring stretching involving the collective oscillation of both Cp rings towards the metal, which is here found to be significantly influenced when the Fc moiety is attached to the polymer chain in PVFc. One could speculate that this mode is, due to its large collective displacement, particularly sensitive to the local environment and extremely broadened in the amorphous polymer.

We now come to the polymers PFDMS and PFMS where the ferrocene complex is part of the polymer backbone itself (see figure 1). Their vibrational spectra are shown in top part of figure 2 and are scaled in intensity to overlap in the low frequency range $\omega < 100 \text{ cm}^{-1}$ and around the broad peak at $800\text{--}900 \text{ cm}^{-1}$. For PFDMS, two molecular weights of 16 and 88 kg mol^{-1} were investigated. Assuming that the latter broad peak is governed by internal modes of the ferrocene complex, this corresponds to a normalization to the number of monomer units. In this representation, it is obvious that the spectra of PFDMS16 and PFDMS88 are identical and independent of the molecular weight. The spectrum of PFMS differs mostly in the

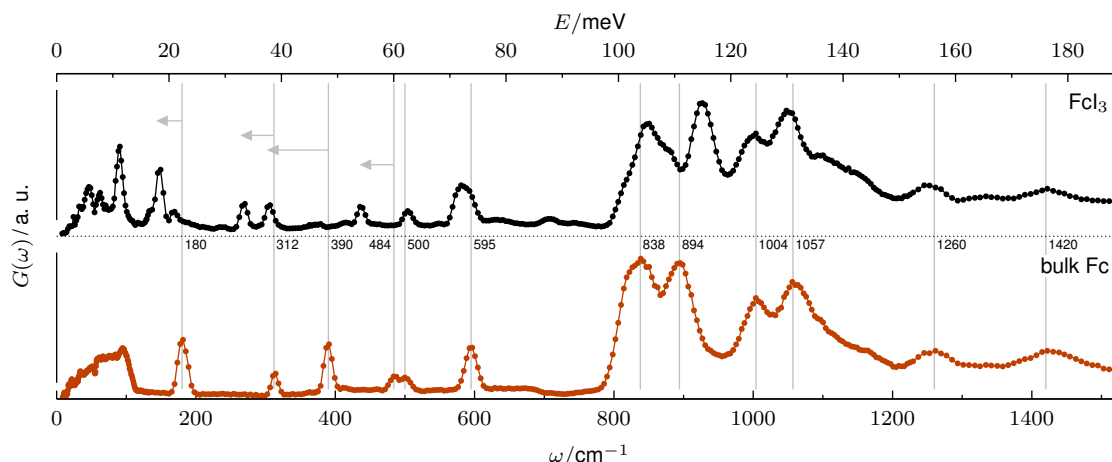


Figure 3. Experimental generalized density of states $G(\omega)$ for triclinic ferrocene (Fc), and ferrocenium triiodide (FcI_3). All spectra were recorded at $T = 10$ K. Vertical lines show characteristic maxima of the Fc spectrum for easier comparison (ω given in cm^{-1}).

range $100\text{--}300\text{ cm}^{-1}$ where the broad peak structure is less intense, but of similar shape.

As the only difference in the chemical structure of PFMS and PFDMS is the number of methyl groups per monomer, this supports the conclusion that the torsional mode of the methyl groups contributes in this frequency region. A comparison with poly(dimethylsiloxane) (PDMS) [35, 36] shows that the mode around 140 cm^{-1} might be ascribed to the methyl group torsional mode, followed by the 180 cm^{-1} ring-metal-ring bending mode of ferrocene which is shifted to lower frequency.

Moreover, the spectrum of PDMS as discussed by Jayes *et al.* [35] helps to assign the newly appearing peaks at 680 and 745 cm^{-1} (arrows in the top part of figure 2) in PFDMS and PFMS to CH_3 rocking modes. However, we may expect a decreased intensity of these modes in PFMS due to the reduced number of methyl groups which is not the case for the right peak at 745 cm^{-1} .

Concerning the characteristic modes of the ferrocene complex, we find for PFDMS and PFMS instead of a single ring-metal-ring stretching mode at 312 cm^{-1} a symmetrically split double peak – the same holds for symmetric ring tilt at 390 cm^{-1} . We can imagine that the breaking of the rotational symmetry of the Fc complex caused by inclusion in the polymer backbone leads to a splitting of the vibrational modes.

At higher frequencies, the two peaks at 1004 and 1057 cm^{-1} in bulk Fc merge to a single peak in PFDMS and PFMS. They correspond to C–H bending modes in the Cp ring plane which are expected to be strongly modified when the ferrocene molecule is bound as part of a polymer chain.

3.2. Oxidized compounds

In addition to ferrocene and ferrocene-containing polymers, we studied the oxidized compounds FcI_3 and PVFcI_x in order to investigate the influence of oxidation on the ferrocene complex. Figure 3 shows the comparison of bulk Fc with FcI_3 . Both substances are in a crystalline phase. The low energy part of the spectrum $< 100\text{ cm}^{-1}$ shows several sharp peaks for FcI_3 . One can speculate that this peak structure is caused by optical phonon branches corresponding to low energy out-of-phase vibrations of the Fc^+ and I_3^- molecules. The remaining modes between 180 and 484 cm^{-1} differ significantly in FcI_3 with respect to Fc. It is consistent with the expectation that the weakening of the ferrocenium ion by a missing electron leads to a shift

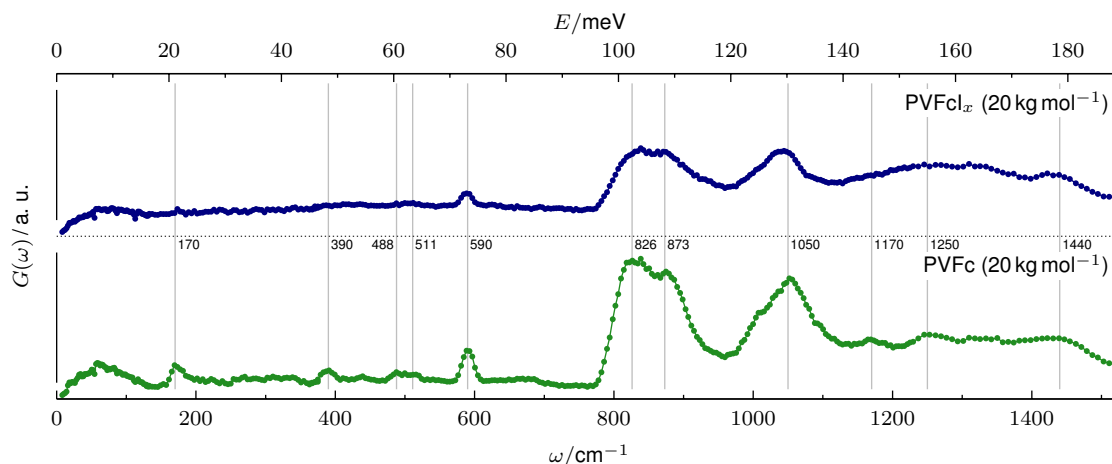


Figure 4. Experimental generalized density of states $G(\omega)$ for poly(vinylferrocene) (PVFc), and poly(vinylferrocene) oxidized with iodine (PVFcI_x). All spectra were recorded at $T = 10$ K. Vertical lines show characteristic maxima of the PVFc spectrum for easier comparison (ω given in cm^{-1}).

to lower frequencies for internal modes involving the η^5 -complex bond. The grey arrows in the figure give a possible assignment of the modes undergoing a shift. Modes at higher frequencies involving deformation of the Cp rings show less differences, with the exception of the peak at 894 cm^{-1} . A more detailed study and phonon calculations of FcI₃ will certainly help in giving the correct assignment and interpretation of the influence of oxidation on the vibrational spectrum of ferrocene. This work is currently in progress.

In contrast to Fc and FcI₃, the comparison of the ferrocene-containing polymer PVFc and its iodine oxidized compound PVFcI_x shown in figure 4 exhibits significantly less detail. For the oxidized polymer, the background is much higher and aside from the broad ring deformation modes above 800 cm^{-1} which are left mostly uninfluenced by the oxidation, only the out of plane ring deformation mode at 590 cm^{-1} is distinguishable in the spectrum of PVFcI_x. This mode is, as in the case of FcI₃, not shifted with respect to the unoxidized compound. The peak at 170 cm^{-1} corresponding to ring-metal-ring bending with antisymmetric ring tilt is not distinguishable in the spectrum of PVFcI_x anymore – the comparison of Fc and FcI₃ has already shown that this mode is significantly shifted to lower frequencies and is thus probably not separable from the low energy excitations.

4. Conclusion

The use of inelastic neutron spectroscopy enabled us to investigate the vibrational spectrum of the ferrocene complex in different redox-responsive ferrocene-containing polymers. When the ferrocene moiety is attached as a side group as in PVFc, we found significant broadening of the ring-metal-ring bending with antisymmetric ring tilt and no sign of the ring-metal-ring stretching mode. With these exceptions, no shift of the vibrational fingerprint modes in the range $100\text{--}800 \text{ cm}^{-1}$ was detected.

In contrast to this, a more dramatic influence on the vibrational modes was observed when the ferrocene is part of the polymer backbone as in PFDMS. The interpretation of these data is complicated by significant contributions from methyl groups of the polymer. However, the study of PFMS and comparison to previous results for PDMS helped in identifying methyl group torsion contributions.

In case of oxidation of the ferrocene complex, the weakening of the coordination bond in FcI_3 leads to a significant shift of multiple fingerprint modes to lower frequencies. A DFT study to substantiate this observation and give an unambiguous assignment of the modes is currently in progress.

Acknowledgments

The Institut Laue-Langevin (Grenoble, France) is acknowledged for the allocation of beamtime on IN1-Lagrange. The authors would like to thank Andreas Weber and Monica Jimenez-Ruiz for their assistance during the experiment. J. E., M. G. and B. S. thank the Landes-Offensive zur Entwicklung Wissenschaftlich-ökonomischer Exzellenz (LOEWE Soft Control) for ongoing financial support of this work.

References

- [1] Stuart M A C, Huck W T S, Genzer J, Müller M, Ober C, Stamm M, Sukhorukov G B, Szleifer I, Tsukruk V V, Urban M, Winnik F, Zauscher S, Luzinov I and Minko S 2010 *Nat. Mater.* **9** 101–13
- [2] Chen T, Ferris R, Zhang J, Ducker R and Zauscher S 2010 *Prog. Polym. Sci.* **35** 94–112
- [3] Hu J, Meng H, Li G and Ibekwe S I 2012 *Smart Mater. Struct.* **21** 053001
- [4] Lee H, Pietrasik J, Sheiko S S and Matyjaszewski K 2010 *Prog. Polym. Sci.* **35** 24–44
- [5] Minko S 2006 *Polym. Rev.* **46** 397–420
- [6] Lallana E and Tirelli N 2013 *Macromol. Chem. Phys.* **214** 143–58
- [7] Ramanathan M, Tseng Y C, Ariga K and Darling S B 2013 *J. Mater. Chem. C* **1** 2080–91
- [8] Abd-El-Aziz A S, Agatemor C and Etkin N 2014 *Macromol. Rapid Commun.* **35** 513–559
- [9] Whittell G R, Hager M D, Schubert U S and Manners I 2011 *Nat. Mater.* **10** 176–88
- [10] Bellas V and Rehahn M 2007 *Angew. Chem., Int. Ed.* **46** 5082–104
- [11] Whittell G and Manners I 2007 *Adv. Mater.* **19** 3439–68
- [12] Manners I 2004 *Synthetic Metal-Containing Polymers* (Weinheim: Wiley)
- [13] Hempenius M A, Cirmi C, Lo Savio F, Song J and Vancso G J 2010 *Macromol. Rapid Commun.* **31** 772–83
- [14] Nakahata M, Takashima Y, Yamaguchi H and Harada A 2011 *Nature Commun.* **2** 511
- [15] Staff R H, Gallei M, Mazurowski M, Rehahn M, Berger R, Landfester K and Crespy D 2012 *ACS Nano* **6** 9042–9
- [16] Elbert J, Gallei M, Rüttiger C, Brunsen A, Didzoleit H, Stühn B and Rehahn M 2013 *Organometallics* **32** 5873–8
- [17] Elbert J, Mersini J, Vilbrandt N, Lederle C, Kraska M, Gallei M, Stühn B, Plenio H and Rehahn M 2013 *Macromolecules* **46** 4255–67
- [18] Elbert J, Krohm F, Rüttiger C, Kienle S, Didzoleit H, Balzer B N, Hugel T, Stühn B, Gallei M and Brunsen A 2013 *Adv. Funct. Mater.* **24** 1591–1601
- [19] Rider D A and Manners I 2007 *Polym. Rev.* **47** 165–95
- [20] Ahmed R, Priimagi A, Faul C F J and Manners I 2012 *Adv. Mater.* **24** 926–31
- [21] Schacher F H, Elbert J, Patra S K, Yusoff S F M, Winnik M A and Manners I 2012 *Chem.–Eur. J.* **18** 517–25
- [22] Schacher F H, Bellas V, Winnik M A and Manners I 2013 *Soft Matter* **9** 8569–78
- [23] Zhang M, Rupar P A, Feng C, Lin K, Lunn D J, Oliver A, Nunns A, Whittell G R, Manners I and Winnik M A 2013 *Macromolecules* **46** 1296–304

- [24] Tonhauser C, Mazurowski M, Rehahn M, Gallei M and Frey H 2012 *Macromolecules* **45** 3409–18
- [25] Morsbach J, Natalello A, Elbert J, Winzen S, Kroeger A, Frey H and Gallei M 2013 *Organometallics* **32** 6033–9
- [26] Kraska M, Gallei M, Stühn B and Rehahn M 2013 *Langmuir* **29** 8284–91
- [27] Gallei M, Schmidt B V K J, Klein R and Rehahn M 2009 *Macromol. Rapid Commun.* **30** 1463–9
- [28] Schmidt B V K J, Elbert J, Barner-Kowollik C and Gallei M 2014 *Macromol. Rapid Commun.* **35** 708–714
- [29] Kemner E, de Schepper M, Kearley G and Jayasooriya U 2000 *J. Chem. Phys.* **112** 10926–29
- [30] Kemner E, Overweg A R, Jayasooriya U A, Parker S F, de Schepper I M and Kearley G J 2002 *Appl. Phys. A: Mater. Sci. Process.* **74** S1368–S1370
- [31] Gallei M, R Klein R and Rehahn M 2010 *Macromolecules* **43** 1844–54
- [32] Kloninger C and Rehahn M 2004 *Macromolecules* **37** 1720–7
- [33] Du V A and Manners I 2013 *Macromolecules* **46** 4742–53
- [34] Lovesey S 1984 *Theory of Neutron Scattering from Condensed Matter (International Series of Monographs on Physics vol 1)* (Oxford: Clarendon Press)
- [35] Jayes L, Hard A P, Séné C, Parker S F and Jayasooriya U A 2003 *Anal. Chem.* **75** 742–6
- [36] Hard A P, Parker S F and Jayasooriya U A 2007 *Appl. Spectrosc.* **61** 314–20